

This article was downloaded by: [University Of Maryland]

On: 17 October 2014, At: 12:05

Publisher: Taylor & Francis

Informa Ltd Registered in England and Wales Registered Number: 1072954 Registered office: Mortimer House, 37-41 Mortimer Street, London W1T 3JH, UK



Combustion Science and Technology

Publication details, including instructions for authors and subscription information:

<http://www.tandfonline.com/loi/gcst20>

Initiation and Reaction in Al/Bi₂O₃ Nanothermites: Evidence for the Predominance of Condensed Phase Chemistry

Nicholas W. Piekieł^a, Lei Zhou^a, Kyle T. Sullivan^a, Snehaunshu Chowdhury^a, Garth C. Egan^a & Michael R. Zachariah^a

^a Department of Chemical and Biomolecular Engineering and Department of Chemistry and Biochemistry, University of Maryland, College Park, Maryland, USA

Accepted author version posted online: 05 Jun 2014. Published online: 23 Jul 2014.

To cite this article: Nicholas W. Piekieł, Lei Zhou, Kyle T. Sullivan, Snehaunshu Chowdhury, Garth C. Egan & Michael R. Zachariah (2014) Initiation and Reaction in Al/Bi₂O₃ Nanothermites: Evidence for the Predominance of Condensed Phase Chemistry, *Combustion Science and Technology*, 186:9, 1209-1224, DOI: [10.1080/00102202.2014.908858](https://doi.org/10.1080/00102202.2014.908858)

To link to this article: <http://dx.doi.org/10.1080/00102202.2014.908858>

PLEASE SCROLL DOWN FOR ARTICLE

Taylor & Francis makes every effort to ensure the accuracy of all the information (the "Content") contained in the publications on our platform. However, Taylor & Francis, our agents, and our licensors make no representations or warranties whatsoever as to the accuracy, completeness, or suitability for any purpose of the Content. Any opinions and views expressed in this publication are the opinions and views of the authors, and are not the views of or endorsed by Taylor & Francis. The accuracy of the Content should not be relied upon and should be independently verified with primary sources of information. Taylor and Francis shall not be liable for any losses, actions, claims, proceedings, demands, costs, expenses, damages, and other liabilities whatsoever or howsoever caused arising directly or indirectly in connection with, in relation to or arising out of the use of the Content.

This article may be used for research, teaching, and private study purposes. Any substantial or systematic reproduction, redistribution, reselling, loan, sub-licensing, systematic supply, or distribution in any form to anyone is expressly forbidden. Terms &

Conditions of access and use can be found at <http://www.tandfonline.com/page/terms-and-conditions>

INITIATION AND REACTION IN Al/Bi₂O₃ NANOTHERMITES: EVIDENCE FOR THE PREDOMINANCE OF CONDENSED PHASE CHEMISTRY

Nicholas W. Piekielek, Lei Zhou, Kyle T. Sullivan, Snehaunshu Chowdhury, Garth C. Egan, and Michael R. Zachariah

Department of Chemical and Biomolecular Engineering and Department of Chemistry and Biochemistry, University of Maryland, College Park, Maryland, USA

This study explores the reaction between Al and Bi₂O₃ nanoparticles under high heating rate conditions with temperature-jump/time of flight mass spectrometry (T-Jump/TOFMS), high speed imaging, and rapid sample heating within a scanning electron microscope (SEM). Comparison of rapid heating of Al/Bi₂O₃ thermite and neat Bi₂O₃ shows that initiation of the Al/Bi₂O₃ reaction occurs at a much lower temperature than the point where oxygen is released from the neat Bi₂O₃ powder. Thus, without the presence of a gas phase oxidizer, it can be concluded that a condensed phase initiation mechanism must be at play in the Al/Bi₂O₃ nanothermite. C/Bi₂O₃ heating experiments were used for a mechanistic comparison between two different fuel types since the carbon represents a nonvolatile fuel in contrast to the aluminum. This formulation showed a similar condensed phase initiation as was seen with the aluminum nanothermite. Qualitative comparison of high speed imaging for Al/Bi₂O₃ and Al/CuO indicates that the initiation reaction in Al/Bi₂O₃ is about twice as fast as a comparable copper oxide system, which has not been apparent from bulk thermite combustion studies. Bi₂O₃ is known to possess unique ion transport properties, which combined with the presence of oxygen and aluminum ions within the nanothermite system may play a significant role in the speed of the nanothermite reaction.

Keywords: Bismuth oxide; Condensed phase reaction; Mass spectrometry; Nanothermite; Rapid heating

INTRODUCTION

Thermite reactions are gaining interest in the field of energetic materials (EMs) due to high energy densities and adiabatic flame temperatures, which are comparable to, or greater than those of traditional organic based energetics (e.g., RDX). Unlike organic EMs, nanothermite performance is easily tuned through variations in stoichiometry, packing density, or oxidizer composition. However, due to large characteristic diffusion length scales, traditional thermites burn at a much slower rate than those of organic energetics that have the fuel and oxidizer mixed at the molecular level. Nanothermites are

Received 27 March 2012; revised 19 March 2014; accepted 24 March 2014.

Address correspondence to Michael R. Zachariah, Department of Mechanical Engineering, University of Maryland, 2125 Martin Hall, College Park, MD 20742, USA. E-mail: mrz@umd.edu

Color versions of one or more of the figures in the article can be found online at www.tandfonline.com/gcst.

most commonly comprised of aluminum (fuel) and metal oxide particles with primary sizes <100 nm. Reduced lengths scales, implying decreased diffusion lengths, help nanothermites to demonstrate burn rates up to several orders of magnitude higher than comparable microscale thermites (Dutro et al., 2009; Levitas et al., 2008; Puszynski, 2009; Shimojo et al., 2009; Son et al., 2007).

Given the central role that nanoaluminum plays in the nanothermite reaction, much attention has been given to understanding the transport of metallic aluminum with respect to its inherent Al_2O_3 shell. The exact nature of aluminum transport is not known, but several models have been proposed, including aluminum and oxygen diffusion through the alumina shell (Dreizin, 1999; Rai et al., 2006; Trunov et al., 2006), pressure build up due to melting of the aluminum, which ruptures the shell allowing Al to leak out (Rosenband, 2004), and extreme pressure build up causing eruption of the alumina shell that spallates the molten aluminum (Levitas et al., 2006). Regardless of the argument, it can be agreed that rapid heating of an aluminum particle will have a positive effect on the transport of aluminum.

In recent studies, interest has shifted towards understanding the effect of different oxidizers on the nanothermite reaction (Martirosyan et al., 2009b; Sanders et al., 2007; Zhou et al., 2010). Because of the large variety of metal oxides available, each with different physical, chemical, and electrical properties, the potential to change the energy release profile becomes feasible. One metal oxide of particular interest is bismuth trioxide (Bi_2O_3), which has a relatively low vapor pressure and unique conducting properties at higher temperatures. Bi_2O_3 is well known as a good oxide ion conductor, and has been extensively researched for use in electrochemical cell applications (Hull et al., 2009; Ivetic et al., 2007; Sabioni et al., 2008; Shuk et al., 1996; Takahashi et al., 1977). The δ -phase of Bi_2O_3 , which is stable from 1002–1097 K (Shuk et al., 1996; Takahashi et al., 1977), shows an advanced ion conductivity up to two orders of magnitude greater than that of its other phases (Hull et al., 2009). Since this phenomenon occurs close to the point of aluminum melting, an important mechanistic step of the nanothermite reaction, this may be significant to the reaction.

When nanoscale Bi_2O_3 is combined with aluminum nanoparticles, a very reactive system is formed (Martirosyan, 2011; Martirosyan et al., 2009a; Sanders et al., 2007; Wang et al., 2011; Williams et al., 2013). Sanders et al. (2007) investigated the difference between four aluminum nanothermites: Al/CuO, Al/ Bi_2O_3 , Al/ MoO_3 , and Al/ WO_3 . Each of these thermite mixtures was subjected to tests in a closed bomb pressure cell, open tray burn, and burn tube. Their results show that Al/ Bi_2O_3 produces the largest peak and average pressure, consistent with other experimental work (Williams et al., 2013), and equilibrium calculations that indicate it produces the most gaseous species during combustion when compared to other oxidizers (Martirosyan et al., 2009b; Puszynski et al., 2007; Sanders et al., 2007). However, Al/ Bi_2O_3 is reported to have the lowest propagation velocity in burn tube experiments and a slightly lower propagation rate than Al/CuO in the open tray experiments (Sanders et al., 2007). Contrary results were seen in open tray experiments by Puszynski et al. (2007) where Al/ Bi_2O_3 produced higher burn rates than Al/CuO, Al/ MoO_3 , or Al- WO_3 . This study by Puszynski and coworkers also included differential scanning calorimetry (DSC) at slow heating rates of 1–20 K/min, and showed the peak of the exotherm to be in the range of ~ 839 – 861 K depending on the size of the Bi_2O_3 particles. A recent study on Al/ Bi_2O_3 and its dependence on aluminum particle size and Al_2O_3 shell thickness was performed by Wang et al. (2011). They observe a burn rate nearly 30 times greater with nanoaluminum, relative to aluminum with a $70\text{-}\mu\text{m}$ primary particle size. Measured ignition temperatures were between 749–797 K for heating rates of

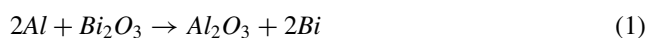
53.4–92.5 K/min. Williams et al. (2013) observed a similar ignition temperature range for fully-dense Al/Bi₂O₃ of 650–800 K for a heating rate range of 200–2000 K/s.

These prior relevant works have probed the reactivity of Al/Bi₂O₃ and its dependence on morphology, environment, etc. with mixed results, but have typically not identified the initial mechanism for reaction. Our group has several previous studies characterizing nanothermite reactions (Chowdhury et al., 2010; Sullivan et al., 2009, 2010, 2011; Zhou et al., 2009a, 2010), including one that highlights the role of oxygen release, and its relationship to ignition temperature and ignition delay (Zhou et al., 2010). In a more comprehensive study, we found that depending on the metal oxide employed, ignition could occur after O₂ release, before O₂ release, and without O₂ release (Jian et al., 2013). We have also investigated the formation of ionic species during the nanothermite reaction in Al/Bi₂O₃, Al/CuO, Al/Fe₂O₃, and Al/WO₃, demonstrating that the bismuth oxide thermite produces the highest rate of ion release (Zhou et al., 2009a), although its relationship to ignition is still unclear. More recently, we proposed that nanothermites undergo a ‘reactive sintering’ mechanism when subjected to rapid heating (Sullivan et al., 2010, 2012). During reactive sintering, initiation of the reaction occurs in the condensed-phase at points of interfacial contact. As heat is generated by the reaction, it is conducted to neighboring particles, further inducing melting and rapidly increasing the intimate contact at the reacting surface. Work on fully-dense thermite systems, including Al/Bi₂O₃ by Williams et al. (2012, 2013), found a similar initial reaction mechanism. They predict that a condensed phase reaction occurs prior to thermal runaway of the thermite reaction to form metastable metal oxides that better transport heat and produce gaseous O₂ to further promote the thermite reaction.

The present study investigates the initial Al/Bi₂O₃ nanothermite reactions with a variety of diagnostic tools at heating rates of more than 10⁵ K/s. Because of the interesting and in some cases contradictory behavior of the Bi₂O₃ nanocomposites, and the lack of mechanistic studies at high heating rates, we present our results for time resolved temperature-jump mass spectrometry and temperature-jump scanning electron microscopy (SEM). C/Bi₂O₃ was examined to further probe the fuel/oxidizer interaction under conditions where the fuel in this case is nonvolatile. Select experiments were repeated with Al/CuO and Al/Bi₂O₃/CuO, as Al/CuO has been shown to be a comparable thermite reaction in several previous studies (Puszynski et al., 2007; Sanders et al., 2007; Williams et al., 2013). The use of Al/Bi₂O₃/CuO allows for a mechanistic view of the competition between the two metal oxides to promote the thermite reaction. The results for C/Bi₂O₃, Al/Bi₂O₃, Al/CuO, and Al/Bi₂O₃/CuO are directly compared to draw some conclusions about the governing mechanisms in each system. Analysis suggests that Bi₂O₃ is indeed unique in that it clearly demonstrates the ability to rapidly initiate a reaction in the condensed phase, and provides further evidence towards a condensed state ‘reactive sintering’ mechanism.

EXPERIMENTAL

Nanothermite samples were stoichiometrically mixed using aluminum, Bi₂O₃, and CuO nanoparticles following the formulas:



where the primary particle size for Bi_2O_3 (Sigma-Aldrich), CuO (Sigma-Aldrich), and aluminum (Argonide Corp.) as specified by the manufacturers were ~ 100 nm, < 50 nm, and ~ 50 nm, respectively. $\text{C}/\text{Bi}_2\text{O}_3$ samples were stoichiometrically mixed assuming:



with “regal 300” carbon black (Cabot Corp.), which has a primary particle size of ~ 50 nm (determined by SEM). While calculating stoichiometry, the inherent Al_2O_3 shell on the aluminum nanoparticle was considered. The shell was taken to be 30% of the mass as previously determined through gravimetric analysis. The samples were initially placed in a hexane solution and were sonicated for ~ 20 min to ensure a fine mixing of materials.

The primary experimental tool is a temperature-jump/time-of flight mass spectrometer (T-Jump/TOFMS) (Zhou et al., 2009b). In brief, the sample slurry is coated on an ~ 1 -cm-long, $76\text{-}\mu\text{m}$ diameter platinum filament, which can be heated at a rate of up to 10^6 K/s with the use of a tunable voltage pulse from an in-house built power supply. The T-Jump filament is inserted directly into the vacuum chamber, close to the electron ionization region of a custom time-of-flight mass spectrometer. This allows for a very short delay (~ 20 μs) between product species evolution, ionization, and subsequent detection by the micro-channel plate (MCP) detector of the TOFMS. Ionization of the gaseous product species is performed by an electron ionization (EI) source with an energy of 70 eV. For a typical heating event, a sequence of 95 spectra with m/z (mass to charge ratio) up to 400 are recorded with a temporal resolution of 100 μs . During heating, the current and voltage through the filament are simultaneously recorded to determine the filament temperature with an uncertainty of ± 40 K. Select T-Jump experiments were also conducted using simultaneous high speed imaging at a rate of $\sim 33,000$ fps with a Phantom 12.1 camera. A heating holder (Protochips, Inc.) was used to visually investigate the morphological changes of Bi_2O_3 inside a scanning electron microscope (SEM; Hitachi SU-70). This holder provides rapid heating of the sample within the SEM, from room temperature to a maximum of 1473 K, at a rate of 10^6 K/s. Images from before and after the heating event can be compared to draw conclusions of how the reaction occurred. In the context of the mass-spectrometry results we consider this as “T-Jump microscopy.”

RESULTS AND DISCUSSION

T-Jump Mass Spectrometry

The rapid heating rates used in both the T-Jump microscopy and T-Jump/TOFMS, as well as the rapid sampling rates of in situ spectrometry, allow for the probing of the initial events of the thermite reaction under heating conditions comparable to those seen in real-time combustion events. To gain a better understanding of each material’s role in a nanocomposite reaction, the $\text{Al}/\text{Bi}_2\text{O}_3$ and $\text{C}/\text{Bi}_2\text{O}_3$ samples as well as neat carbon, aluminum, and bismuth trioxide samples were each tested with the T-Jump/TOFMS. Our primary interest is the $\text{Al}/\text{Bi}_2\text{O}_3$ nanothermite for energetic applications, but the $\text{C}/\text{Bi}_2\text{O}_3$ system offers a valuable mechanistic perspective as aluminum and carbon are very different with respect to their phase changes at the temperature regime of this experiment. Analysis begins with the time resolved mass spectra of the reaction products from rapid heating of $\text{Al}/\text{Bi}_2\text{O}_3$ and neat Bi_2O_3 nanopowders. For each case the heating rate was set to $\sim 3 \times 10^5$ K/s producing a final temperature of ~ 1320 K. A typical spectrum obtained during

Bi₂O₃ heating is shown in Figure 1. Decomposition products include m/z 32 (O₂⁺), m/z 44 (CO₂⁺), m/z 104.5 (Bi⁺²), m/z 209 (Bi⁺), and m/z 226 (BiOH⁺). A full time-resolved set of spectra of the Al/Bi₂O₃ reaction is shown in Figure 2 where the initiation of the reaction occurs at ~ 870 K. The spectrum at $t = 1.8$ ms represents the TOFMS background signal with a major peak at m/z 18, (H₂O⁺) and minor peaks at m/z 17, 28, and 32, representing OH⁺, N₂⁺, and O₂⁺, respectively. The detailed Al/Bi₂O₃ spectrum in Figure 2 shows reaction products of m/z 27 (Al⁺), m/z 70 (Al₂O⁺), m/z 209 (Bi⁺), m/z 104.5 (Bi⁺²), m/z 32 (O₂⁺), and m/z 44 (CO₂⁺). CO₂ production is an unexpected byproduct of our sonication procedure, as residual carbon remains after drying of the nanothermite. The carbon and metal oxide undergo a low temperature reaction producing CO₂ gas as in reaction (3).

The temporal nature of the T-Jump mass-spectrometer experiment allows conclusions to be drawn concerning the initiation steps that may be involved with the bismuth nanothermite reaction, and how it differs from other systems. Figure 3 shows the temporal behavior of select reaction products for Al/Bi₂O₃ and neat Bi₂O₃. If we compare the reaction products in Figure 3 for heating of the thermite (parts A–C) and the neat oxide (parts D–E), we see that there is a clear difference in the time of appearance between thermite ignition, and gas phase O₂ release from the oxide. Although these two samples were tested in separate heating runs, the experimental conditions were replicated in a similar fashion so that qualitative conclusions can be confidently made. During oxide heating (parts D and E of Figure 3), Bi and O₂ are released very late at ~ 3.1 ms, but for nanothermite heating, combustion starts at ~ 1.8 ms, as signified by the appearance of Bi, O₂, and shortly after, Al. This is in contrast to Al/CuO, Al/Fe₂O₃, and Al/ZnO (Zhou et al., 2010), for which the thermite reaction initiates at a time and temperature in close proximity to the point of gaseous O₂ release from the neat oxidizer. Although those systems react as gaseous O₂ is released, it does not necessarily prove that gaseous O₂ is required for reaction. At the point of O₂ release, phase changes in the oxidizer also occur and could promote reaction. In comparison to other thermites, Al/Bi₂O₃ shows substantially different reaction characteristics. The late production of gaseous O₂ by Bi₂O₃ implies that initiation of the Al/Bi₂O₃ reaction occurs in the condensed phase.

Despite this evidence of condensed phase reaction, the volatilization of aluminum remains a mechanistic concern. To further investigate this process we consider a fuel which will not change phase (i.e., melt or vaporize) at the temperatures relevant to this experiment. For this purpose, we employed a C/Bi₂O₃ thermite using nanometer scale carbon particles. As with the Al/Bi₂O₃ study, C, Bi₂O₃, and C/Bi₂O₃ were each heated in separate, but consistent experimental runs. Figure 4 displays the CO₂ release and Figure 5 shows O₂ release

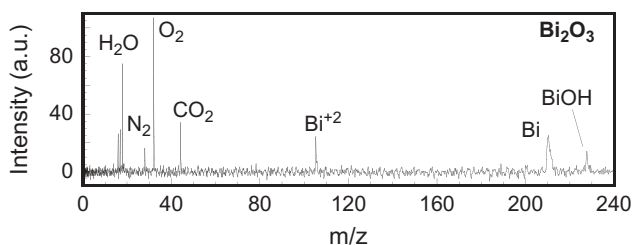


Figure 1 Time-of-flight mass spectrum for Bi₂O₃ sample.

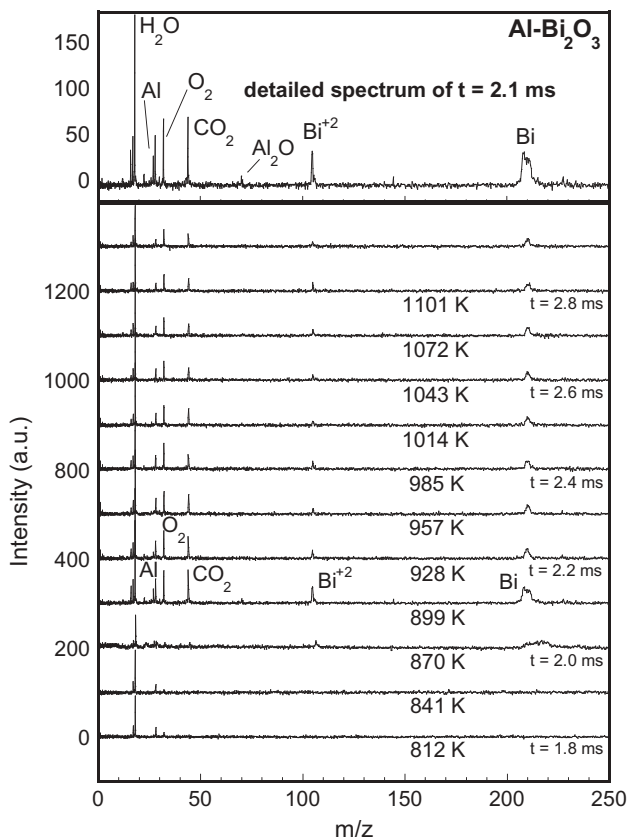


Figure 2 Full spectrum for Al/Bi₂O₃ nanothermite reaction. Each spectrum is separated in time by 100 μ s.

from the carbon, Bi₂O₃ and C/Bi₂O₃ heating experiments. From reaction (3) we expect the C/Bi₂O₃ composite to produce carbon dioxide gas, which is observed in Figure 4. As with Al/Bi₂O₃, the initial point of combustion (time of CO₂ release in Figure 4) occurs well before the point of oxygen release from the bismuth oxide powder seen in Figure 5. There is also essentially no oxygen seen during the C/Bi₂O₃ reaction, suggesting that it is completely consumed in the reaction. We believe this result to be convincing proof of condensed phase initiation in C/Bi₂O₃ and by inference, also Al/Bi₂O₃. Interestingly, the C/Bi₂O₃ reaction starts at a similar temperature as the initiation of the Al/Bi₂O₃ reaction, \sim 900 K. Since we also see CO₂ in the spectrum for ignition of Al/Bi₂O₃ from reaction between Bi₂O₃ and residual carbon, it is possible that the exothermicity of the C/Bi₂O₃ promotes the start of the Al/Bi₂O₃ reaction.

T-Jump Electron Microscopy

The morphological changes of Al/C/Bi₂O₃ reaction were explored using a Protochips rapid heating stage within a SEM. This stage allows imaging of the sample before and after rapid heating without disturbing the sample or exposing it to the environment. The initial study was designed to investigate the reaction between clusters of Al and

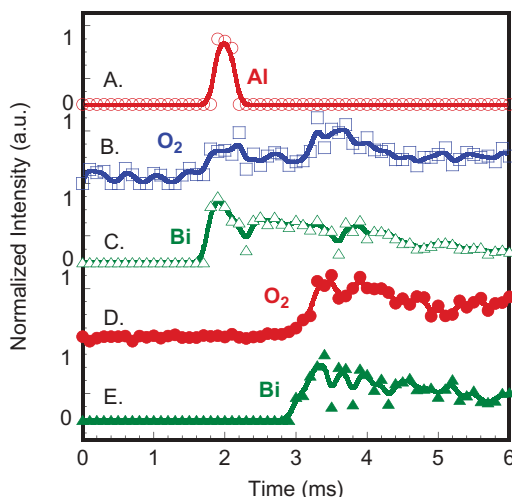


Figure 3 (A)–(C) Products from rapid heating of Al/Bi₂O₃. (D)–(E) Products from rapid heating of neat Bi₂O₃. (A) Al, (B) O₂, (C) Bi, (D) O₂, (E) Bi.

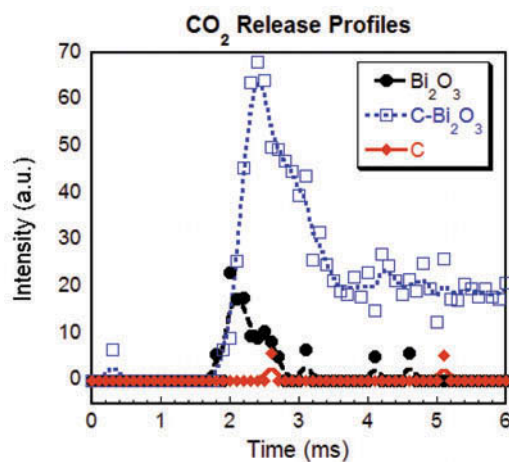


Figure 4 Carbon dioxide release from T-Jump/TOFMS experiments on Bi₂O₃ and C powders, and the C/Bi₂O₃ thermite.

Bi₂O₃ particles, but the particles rest atop a holey carbon film on the SEM grid. A very sparse coating of Al/Bi₂O₃ was applied to the SEM grid, resulting in isolation of Al and Bi₂O₃ as seen in Figure 6. This figure shows a SEM image of the sample on the grid before heating, where the dark background is the thin carbon film and the light, grainy surfaces are holes in the carbon film which expose the underlying silicon carbide. As a result of this sparse particle coating on the few nanometers thick holey carbon film, there is opportunity to study the heating of Al and Bi₂O₃ as well as reactions with the underlying carbon substrate.

The sample was given a heating pulse from room temperature to 1273 K at a rate of 10⁶ K/s and then held for 1 ms; the results of which are shown in Figure 7. In this

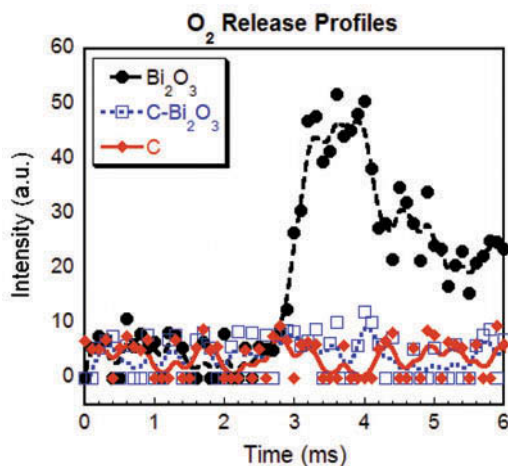


Figure 5 Oxygen release from T-Jump/TOFMS experiments on Bi_2O_3 and C powders, and the C/ Bi_2O_3 thermite.

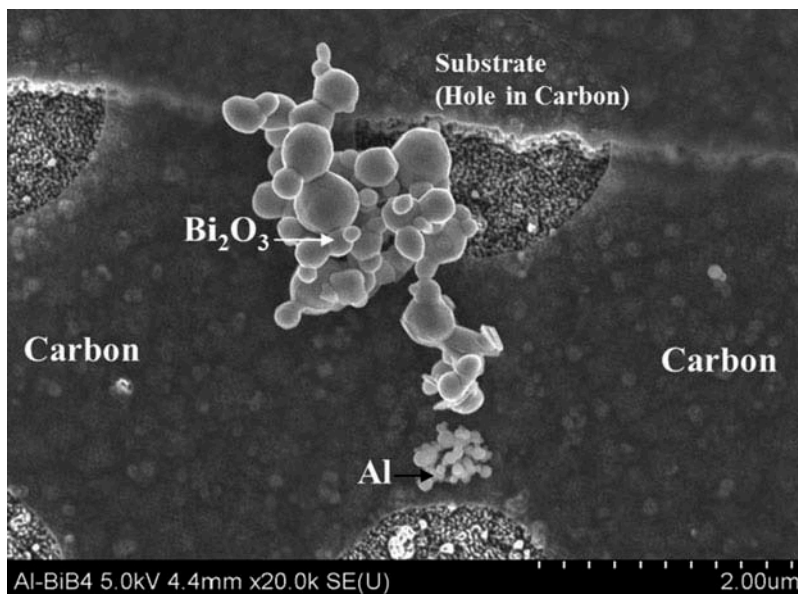


Figure 6 TEM image of bismuth trioxide and aluminum nanoparticles before heating.

figure, significant morphological changes are observed for the Bi_2O_3 particles, but not for the aluminum particles. We conclude that due to the isolation of Al and Bi_2O_3 no reaction was observed between these two components. For each component of this system, the melting temperature of the bulk material is listed in Table 1. Since aluminum melts at 933 K and bismuth trioxide melts at 1097 K, morphological changes in the aluminum were also expected. We assume that the aluminum core is melting but not rupturing the Al_2O_3 shell, which has previously been demonstrated using molecular dynamics simulations (Henz et al., 2010) The morphological changes in the Bi_2O_3 could be due to melting,

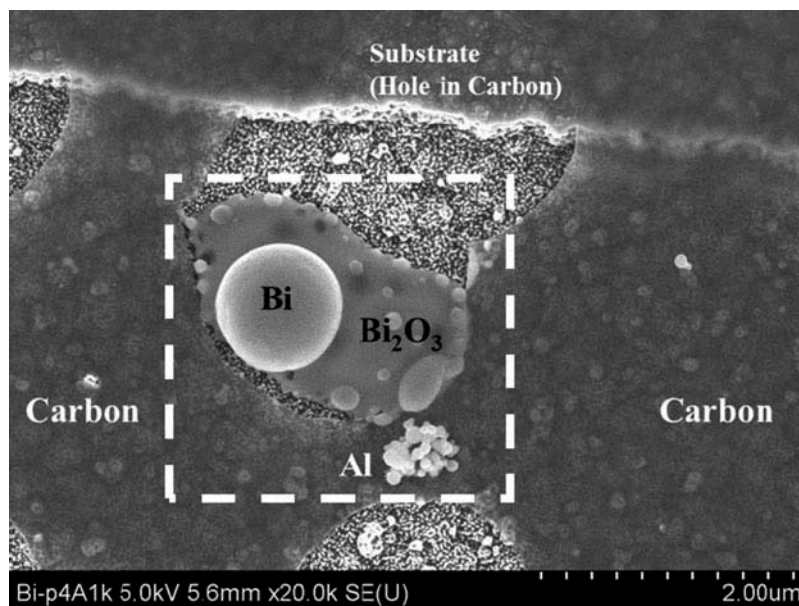


Figure 7 SEM image of Bi₂O₃ and Al particles after heating to 1273 K for 1 ms at a rate of 10⁶ K/s with a high heating rate TEM grid. The dotted box represents the area sampled by EDS shown in Figure 8.

Table 1 Melting and ignition temperature for the various components involved in the nanothermite reaction

Component	Bulk melting temperature (K)	T-Jump ignition temperature of respective Al-nanothermite (K)	T-Jump ignition temperature of respective C-nanothermite (K)
Bi ₂ O ₃	1097 K (Shuk et al., 1996)	870 K	900 K (Piekiel et al., 2012)
CuO	1719 K (Patnaik, 2003)*	1010 K (Sullivan et al., 2012)	900 K (Piekiel et al., 2012)
Fe ₂ O ₃	1838 K (Patnaik, 2003)	1270 K (Sullivan et al., 2012)	1030 K (Piekiel et al., 2012)
WO ₃	1745 K (Patnaik, 2003)	1065 K (Sullivan et al., 2012)	—
Al ₂ O ₃	2345 K (Patnaik, 2003)	—	—
Al	933 K (Patnaik, 2003)	—	—
C	~3973 K (Patnaik, 2003)	—	—

*CuO decomposes at ~1073 K to form Cu₂O (Patnaik, 2003).

or to an exothermic reaction with the carbon film of the SEM grid. In the T-Jump/TOFMS, C/Bi₂O₃ reacts at ~900 K (Piekiel et al., 2012), and therefore it is likely that the morphological changes observed here are affected by an exothermic reaction. Evidence of reaction can be confirmed in Figure 8, which shows elemental analysis of the sample after heating using energy dispersive x-ray spectroscopy (EDS). EDS analysis confirms that during heating of the Bi₂O₃ nanoparticles, a film of Bi₂O₃ is formed over which spheres of Bi reside on its surface. In this case, presumably liquid Bi₂O₃ is reacting with the underlying carbon substrate, which can be seen by the recession of the hole in the carbon film from Figure 6 to Figure 7. The C/Bi₂O₃ reaction occurs via condensed-phase reactions producing gaseous CO₂ and liquid Bi (MP 545 K). The liquid bismuth is immiscible in liquid Bi₂O₃, which promotes phase separation and the formation of large spherical particles of bismuth. This result is consistent with the condensed phase reaction model deduced from the T-Jump/TOFMS experiments.

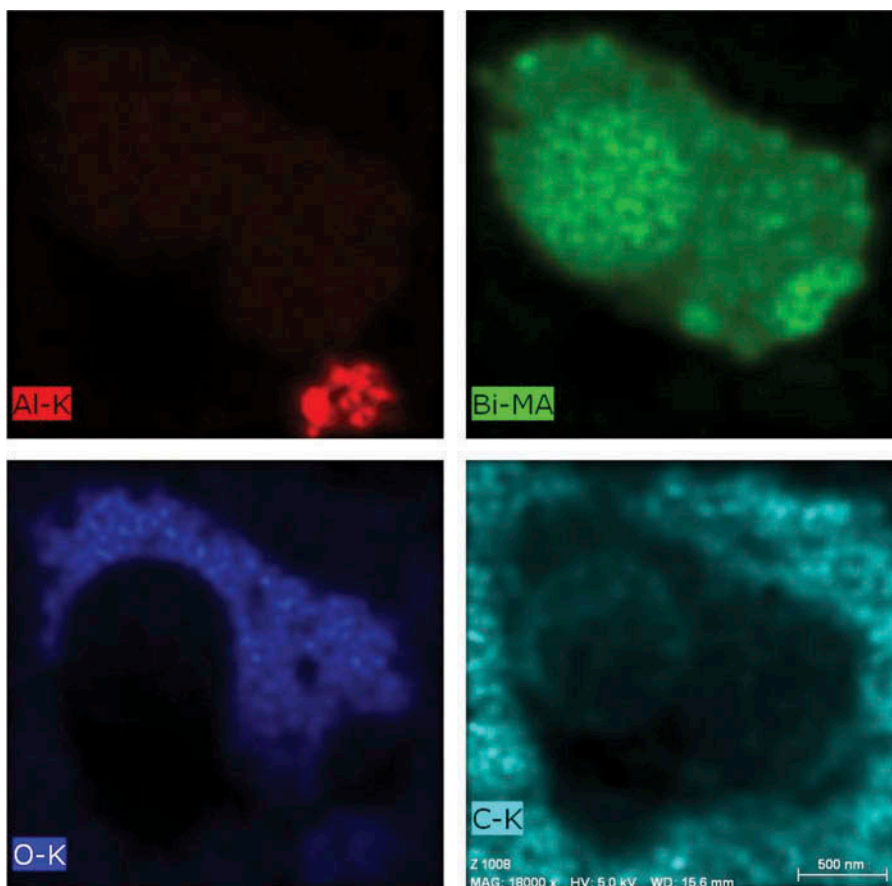


Figure 8 Elemental analysis of boxed region in Figure 7.

Thus far, we have shown evidence of condensed phase reaction during ignition of nanothermites, but it is unclear how $\text{Al}/\text{Bi}_2\text{O}_3$ ignites at 870 K, below the melting point of either bismuth trioxide (1097 K) or aluminum (933 K). In a recent work, with the rapid heating SEM stage, we observed that particle melting is not a necessary prerequisite to initiate a condensed-phase reaction for the Al/WO_3 system (Sullivan et al., 2010). It was seen after heating that WO_3 particles isolated from Al did not undergo any morphological changes. However, in regions where the fuel and oxidizer were intermixed, considerable morphological changes indicative of WO_3 melting were observed. This observation led to speculation that the condensed phase reaction between WO_3 and aluminum initiated below the melting temperature of WO_3 , and then the liberated energy from the exothermic reaction further promoted melting of neighboring WO_3 particles. This effect is called “reactive sintering,” where an initial low temperature condensed phase reaction produces heat to further sinter the surrounding particles (Sullivan et al., 2012). This mechanism is also similar to that proposed by Williams and coworkers for fully-dense thermites (2012, 2013). In the context of this work, a similar mechanism may be occurring and would serve to explain why the $\text{Al}/\text{Bi}_2\text{O}_3$ reaction initiates below the melting point of either constituent.

One potentially useful material property that could help to explain reaction at such a low temperature is the Tammann temperature, which for Bi_2O_3 is ~ 549 K, or half of its

melting point. At a temperature approximately that of the Tammann temperature, nanoparticles can begin to sinter as surface atoms gain a significant amount of mobility (Satterfield, 1991). At lower temperatures this sintering may be minor, but enough to create a junction between particles. For aluminum nanoparticles, morphological changes have been observed at temperatures as low as 863 K, likely due to the crystalline phase shift of the oxide shell from amorphous alumina to γ -Al₂O₃ (Rufino et al., 2007). This alumina phase change can leave gaps in the Al₂O₃ shell resulting in bare Al (Trunov et al., 2006), or sintering of particles that are in contact (Rufino et al., 2007). Therefore, we assume that the surfaces of the aluminum nanoparticles and Bi₂O₃ are both in a liquid-like or “soft” state conducive of mild sintering, at or below the ignition temperature of Al/Bi₂O₃ (870 K). With even a small amount of contact between particles, diffusion of reactive species in the condensed state allows for a reaction to proceed. The added heat from the resulting exothermic reaction accelerates the process as it allows wetting of the Al₂O₃ surface by Bi₂O₃ as occurred in Figure 7 with carbon, and with Al/WO₃ in previous rapid heating experiments (Sullivan et al., 2010). This results in a junction at the Al₂O₃ surface of the aluminum nanoparticles with a greatly increased surface area that allows for enhanced diffusion and reaction of Al and O₂.

High Speed Imaging

For select Al/Bi₂O₃ combustion experiments, high speed imaging was used to capture the reaction within the T-Jump/MS providing a qualitative assessment of the speed of the reaction. For comparison this was also done for Al/CuO, as Al/CuO is a commonly investigated nanothermite and has been previously compared with Al/Bi₂O₃ in larger scale thermite combustion studies. Figures 9 and 10 show select images of the T-Jump experiments under vacuum for Al/Bi₂O₃ and Al/CuO, respectively, at a frame rate of ~33,000 fps. In each figure, the nanothermite-coated platinum filament is in the center of the images, but is not initially visible due to the high frame rate for recording. After initiation of combustion at ~870 K for Al/Bi₂O₃ and ~1010 K for Al/CuO, the reaction propagates along the wire. The Al/CuO reaction typically starts from the edge of the sample, and propagates inward, but the Al/Bi₂O₃ reaction propagates outward. This variation may be due to differences in heat transfer through the powders, but regardless it is evident from the images that under similar heating conditions, Al/Bi₂O₃ undergoes a faster, more violent reaction. While care was taken to qualitatively ensure that the masses for each sample were similar, we are not confident enough on their similarity to extract quantitative burn times. Nevertheless, the images in Figures 9 and 10 present a measurement of the luminous time and allowed an approximation for the burn times for Al/Bi₂O₃ of ~0.08 ms and ~0.18 ms for Al/CuO. This behavior has been consistently observed in other experimental trials, and it is a reasonable assumption that Al/Bi₂O₃ burns about twice as fast as Al/CuO.

Previous burn tube and open tray experiments have given mixed results as to whether Al/CuO or Al/Bi₂O₃ exhibits a higher burn rate due to variations in experimental parameters. Packing density, particle size, tube diameter, and pressure are just a few critical experimental parameters that greatly influence bulk burn rate results. Sanders and coworkers open tray and burn tube flame speed studies (Sanders et al., 2007) show that Al/CuO has the fastest burn rate in open tray experiments followed by Al/Bi₂O₃, while in the burn tube Al/Bi₂O₃ was the poorest performer followed by Al/CuO. However, both the open tray and burn tube experiments are fundamentally different from the current study.

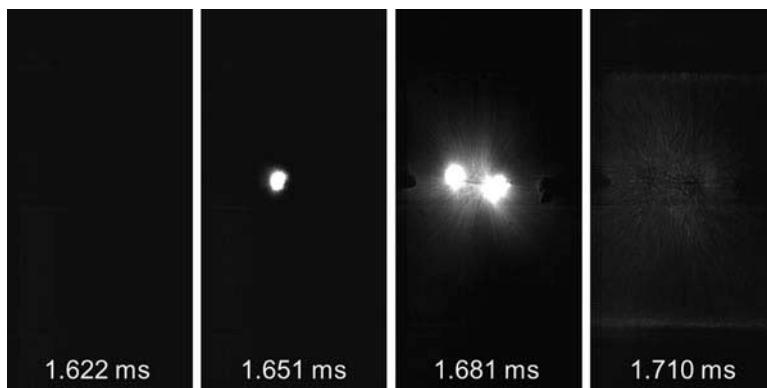


Figure 9 High speed images of Al/Bi₂O₃ during heating in the TOFMS.

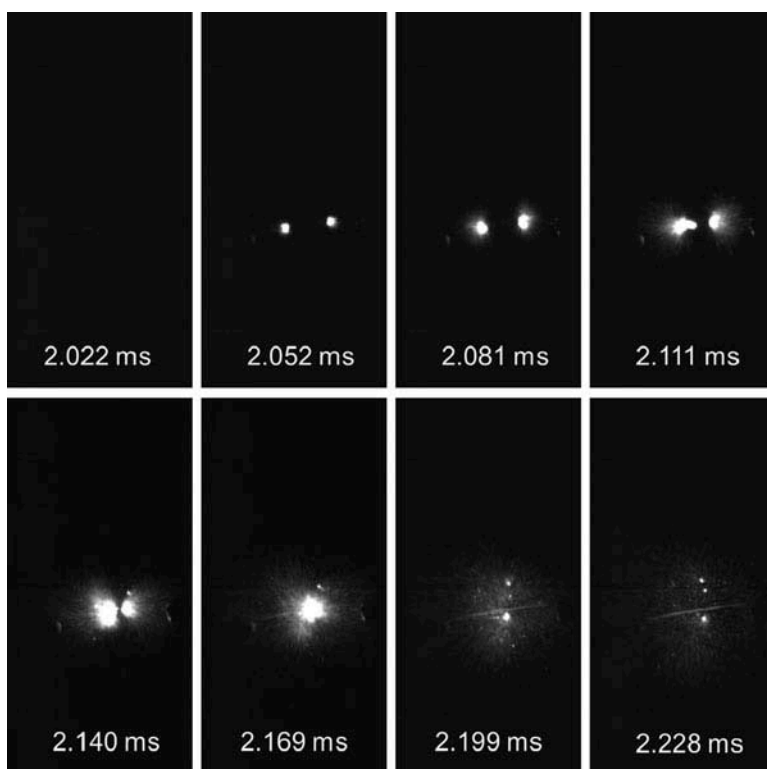


Figure 10 High speed images of Al/CuO during heating in the TOFMS.

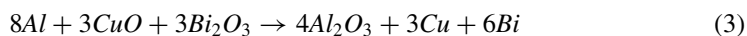
In the current work, we investigate very small samples under high vacuum conditions. This allows for probing of the initial reactions that promote combustion, as opposed to bulk combustion studies at atmospheric pressure that typically probe secondary reactions. Despite poorer performance for Al/Bi₂O₃ versus Al/CuO in bulk combustion studies, our temperature-jump experiments suggest that the opposite is true for the initiation

reactions. It is currently unclear how the rapid initial reaction of Al/Bi₂O₃ affects the bulk mechanism; with the help of future experimental and theoretical work, this information may be a useful mechanistic detail.

Although Figures 9 and 10 show Al/Bi₂O₃ reacting faster than Al/CuO, there is uncertainty as to why this is the case. One feature of the thermite reaction that could be very important is the role of charged particles and inherent electric fields within the thermite mixture, and how they affect diffusion of reactants. With the assumption of a diffusion-limited mechanism, any improvement on the mass transfer process can have a direct impact on reaction speed. Molecular dynamics simulations have been performed showing that electric fields within the aluminum nanoparticle can drive positive aluminum ions through the oxide shell to the outer surface of the particle (Henz et al., 2010). Cabrera and Mott (1948) originally summarized the controlling aspect that inherent electric fields in a thin metal oxide shell (like that of Al₂O₃ in aluminum nanoparticles) have for the oxidation of metals. Their results have been more recently used by Zhdanov and Kasemo (2008) to show that the diffusion rate for Al cations through the oxide shell of Al nanoparticles is greatly enhanced by this local electric field. Ermoline et al. (2012) also leveraged Cabrera and Mott's work to accurately predict the low temperature reaction for Al/CuO. This evidence suggests that positive aluminum ions and the inherent electric field of the Al₂O₃ shell can aid aluminum combustion, but in nanothermite combustion, if the metal oxide can also contribute charged species, the reaction could be enhanced even further. For bismuth trioxide, at 1002 K, just above the ignition point of Al/Bi₂O₃, the oxide can produce and promptly transport negatively charged oxide species (Shuk et al., 1996). This means that as both components (Al and Bi₂O₃) enter a liquid-like state, reactants of opposite charge are produced. Although the Al/Bi₂O₃ reaction begins below the melting point of either Al or Bi₂O₃, the ability of Bi₂O₃ to transport oxide species in the condensed phase may promote the rapid reaction observed in this study. In the past we have experimentally shown an enhanced rate of ion production for Al/Bi₂O₃ compared to other common nanothermites, including Al/CuO (Zhou et al., 2009a). This work also showed that the ion production for Al/Bi₂O₃ occurs at the onset of combustion, implying that the ion production is related to the thermite ignition whether it be as a precursor to ignition or as a player in the mass transport process. The large presence of ionic species and the timing of ion formation combined with the inherent electric field of aluminum particles further support the idea that electric fields have a role in nano-thermite initiation.

Al/CuO/Bi₂O₃

A composite of Al/CuO/Bi₂O₃ was also tested with the high-speed imaging T-Jump/TOFMS setup. This mixture allows a different perspective on how the fuel and oxidizer react and was made stoichiometrically following:



where CuO and Bi₂O₃ are given equal molar quantities. Intuition leads us to predict that this system would ignite at the same temperature as Al/Bi₂O₃, considering Al/Bi₂O₃ ignites at a lower temperature than Al/CuO. We also expect a rapid initial reaction similar to that of Al/Bi₂O₃. This system does begin reaction at the same point as Al/Bi₂O₃, but the reaction lacks the intensity and speed of either Al/CuO or Al/Bi₂O₃ as seen in Figure 11. It is likely

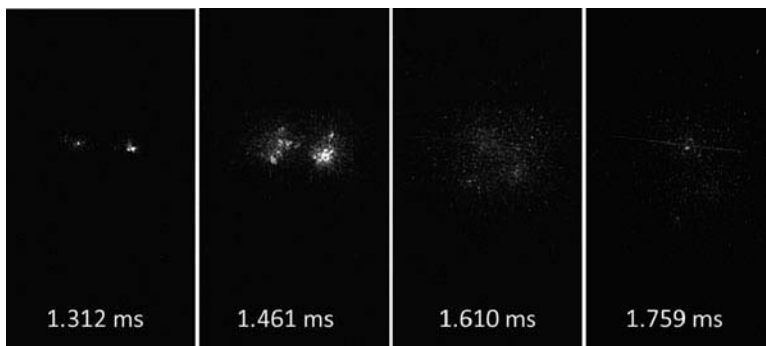


Figure 11 High speed images of Al/CuO/Bi₂O₃ during heating in the TOFMS.

that at the ignition temperature of Al/Bi₂O₃ a fuel rich reaction takes place resulting in poor performance. However, another contribution to poor reactivity of Al/CuO/Bi₂O₃ could be a reaction between the metal oxides. In Figure 7, we observe wetting of the carbon surface by Bi₂O₃, and the same may be occurring between CuO and Bi₂O₃. If we heat CuO/Bi₂O₃ we observe mass-spectral patterns similar to that of neat Bi₂O₃, but with no evidence of CuO decomposition. It is thus possible that aside from reacting with aluminum, the two oxidizers are reacting with each other to form the mixed oxide CuBi₂O₄. This mixed oxide forms at a temperature well below the melting point of either CuO or Bi₂O₃ and is stable up to 1150 K (Kakhan et al., 1979). This result implies that simple mixtures of metal oxides may offer unexpected results due to alloying reactions not only with each other but with the alumina shell (e.g., Alumina + CuO => Al₂CuO₄; Alumina + Bi₂O₃ => Al₄Bi₂O₉). In this case these reactions are detrimental, but no-doubt other combinations of metal oxides may offer different and possibly improved reaction profiles.

CONCLUSION

This study probes the initial reaction events of the Al/Bi₂O₃ nanothermite reaction. In the aforementioned ‘reactive sintering’ study, significant evidence was provided for a condensed state reaction playing an important role in reactions of nanothermites. The current study is a complement to ‘reactive sintering’ and provides definitive evidence that the condensed phase reaction is responsible for ignition of Al/Bi₂O₃. Observation of this event in both Al/Bi₂O₃ and C/Bi₂O₃ further demonstrates that the ability of the oxide to transport its oxidizer is a key feature when considering nanothermite formulations. Although the current study primarily examines Bi₂O₃ containing systems, the evidence for condensed phase reaction demonstrated here, along with the results of the reactive sintering study, suggest that this mechanism is at play for other systems as well.

FUNDING

This work was supported by the Army Research Office and the Defense Threat Reduction Agency. The authors also acknowledge support from the University of Maryland Center for Energetic Concepts Development. We also acknowledge the support of the Maryland NanoCenter and its NispLab. The NispLab is supported in part by the NSF as a MRSEC Shared Experimental Facility.

REFERENCES

- Cabrera, N., and Mott, N.F. 1948. Theory of the oxidation of metals. *Rep. Prog. Phys.*, **12**, 163–184.
- Chowdhury, S., Sullivan, K., Piekiet, N., Zhou, L., and Zachariah, M.R. 2010. Diffusive vs. explosive reaction at the nanoscale. *J. Phys. Chem. C*, **114**, 9191–9195.
- Dreizin, E.L. 1999. On the mechanism of asymmetric aluminum particle combustion. *Combust. Flame*, **117**, 841–850.
- Dutro, G.M., Yetter, R.A., Risha, G.A., and Son, S.F. 2009. The effect of stoichiometry on the combustion behavior of a nanoscale Al/MoO₃ thermite. *Proc. Combust. Inst.*, **32**, 1921–1928.
- Ermoline, A., Stamatis, D., and Dreizin, E.L. 2012. Low-temperature exothermic reactions in fully dense Al–CuO nanocomposite powders. *Thermochim. Acta*, **527**, 52–58.
- Henz, B.J., Hawa, T., and Zachariah, M.R. 2010. On the role of built-in electric fields on the ignition of oxide coated nanoaluminum: Ion mobility versus Fickian diffusion. *J. Appl. Phys.*, **107**, 024901-1–024901-9.
- Hull, S., Norberg, S.T., Tucker, M.G., Eriksson, S.G., Mohn, C.E., and Stolen, S. 2009. Neutron total scattering study of the delta and beta phases of Bi₂O₃. *Dalton Trans.*, **40**, 8737–8745.
- Ivetic, T., Nikolic, M.V., Slankarnenac, M., Zivanov, M., Minic, D., Nikolic, P.M., and Ristic, M.M. 2007. Influence of Bi₂O₃ on microstructure and electrical properties of ZnO–SnO₂ ceramics. *Sci. Sintering*, **39**, 229–240.
- Jian, G., Chowdhury, S., Sullivan, K., and Zachariah, M.R. 2013. Nanothermite reactions: Is gas phase oxygen generation from the oxygen carrier an essential prerequisite to ignition? *Combust. Flame*, **160**, 432–437.
- Kakhan, B.G., Lazarev, V.B., and Shaplygin, I.S. 1979. Subsolidus part of the equilibrium diagrams of the Bi₂O₃–MO binary systems (M = Ni, Cu, or Pd). *Russ. J. Inorg. Chem.*, **24**, 922–925.
- Levitas, V.I., Asay, B.W., Son, S.F., and Pantoya, M. 2006. Melt dispersion mechanism for fast reaction of nanothermites. *Appl. Phys. Lett.*, **89**, 071909.
- Levitas, V.I., Pantoya, M.L., and Dikici, B. 2008. Melt dispersion versus diffusive oxidation mechanism for aluminum nanoparticles: Critical experiments and controlling parameters. *Appl. Phys. Lett.*, **92**, 011921.
- Martirosyan, K.S. 2011. Nanoenergetic gas-generators: Principles and applications. *J. Mater. Chem.*, **21**, 9400–9405.
- Martirosyan, K.S., Wang, L., Vicent, A., and Luss, D. 2009a. Nanoenergetic gas-generators: Design and performance. *Propellants Explos. Pyrotech.*, **34**, 532–538.
- Martirosyan, K.S., Wang, L., Vicent, A., and Luss, D. 2009b. Synthesis and performance of bismuth trioxide nanoparticles for high energy gas generator use. *Nanotechnology*, **20**, 405609.
- Patnaik, P. 2003. *Handbook of Inorganic Chemicals*, McGraw-Hill, New York.
- Piekiet, N.W., Egan, G.C., Sullivan, K.T., and Zachariah, M.R. 2012. Evidence for the predominance of condensed phase reaction in chemical looping reactions between carbon and oxygen carriers. *J. Phys. Chem. C*, **116**, 24496–24502.
- Puszynski, J.A. 2009. Processing and characterization of aluminum-based nanothermites. *J. Therm. Anal. Calorim.*, **96**, 677–685.
- Puszynski, J.A., Bulian, C.J., and Swiatkiewicz, J.J. 2007. Processing and ignition characteristics of aluminum-bismuth trioxide nanothermite system. *J. Propul. Power*, **23**, 698–706.
- Rai, A., Park, K., Zhou, L., and Zachariah, M.R. 2006. Understanding the mechanism of aluminium nanoparticle oxidation. *Combust. Theor. Model.*, **10**, 843–859.
- Rosenband, V. 2004. Thermo-mechanical aspects of the heterogeneous ignition of metals. *Combust. Flame*, **137**, 366–375.
- Rufino, B., Boule'h, F., Coulet, M.V., Lacroix, G., and Denoyel, R. 2007. Influence of particles size on thermal properties of aluminium powder. *Acta Materialia*, **55**, 2815–2827.
- Sabioni, A.C.S., Daniel, A., Ferraz, W.B., Pais, R.W.D., Huntz, A.M., and Jomard, F. 2008. Oxygen diffusion in Bi₂O₃-doped ZnO. *Mater. Res. Ibero-Am. J. Mater.*, **11**, 221–225.

- Sanders, V.E., Asay, B.W., Foley, T.J., Tappan, B.C., Pacheco, A.N., and Son, S.F. 2007. Reaction propagation of four nanoscale energetic composites (Al/MoO₃, Al/WO₃, Al/CuO, and Bi₂O₃). *J. Propul. Power*, **23**, 707–714.
- Satterfield, C.N. 1991. *Heterogeneous Catalysis in Industrial Practice*, 2nd edition, McGraw Hill, New York.
- Shimojo, F., Nakano, A., Kalia, R.K., and Vashishta, P. 2009. Enhanced reactivity of nanoenergetic materials: A first-principles molecular dynamics study based on divide-and-conquer density functional theory. *Appl. Phys. Lett.*, **95**, 043114.
- Shuk, P., Wiemhofer, H.D., Guth, U., Gopel, W., and Greenblatt, M. 1996. Oxide ion conducting solid electrolytes based on Bi₂O₃. *Solid State Ionics*, **89**, 179–196.
- Son, S.F., Yetter, R.A., and Yang, V. 2007. Introduction: Nanoscale composite energetic materials. *J. Propul. Power*, **23**, 643–644.
- Sullivan, K.T., Chiou, W.A., Fiore, R., and Zachariah, M.R. 2010. In situ microscopy of rapidly heated nano-Al and nano-Al/WO₃ thermites. *Appl. Phys. Lett.*, **97**, 133104–133106.
- Sullivan, K.T., Piekielek, N.W., Chowdhury, S., Wu, C., Zachariah, M.R., and Johnson, C.E. 2011. Ignition and combustion characteristics of nanoscale Al/AgIO₃: A potential energetic biocidal system. *Combust. Sci. Technol.*, **183**, 285–302.
- Sullivan, K.T., Piekielek, N.W., Wu, C., Chowdhury, S., Kelly, S.T., Hufnagel, T.C., Fezzaa, K., and Zachariah, M.R. 2012. Reactive sintering: An important component in the combustion of nanocomposite thermites. *Combust. Flame*, **159**, 2–15.
- Sullivan, K., Young, G., and Zachariah, M.R. 2009. Enhanced reactivity of nano-B/Al/CuO MICs. *Combust. Flame*, **156**, 302–309.
- Takahashi, T., Esaka, T., and Iwahara, H. 1977. Oxide ion conduction in sintered oxides of Moo₃-doped Bi₂O₃. *J. Appl. Electrochem.*, **7**, 31–35.
- Trunov, M.A., Schoenitz, M., and Dreizin, E.L. 2006. Effect of polymorphic phase transformations in alumina layer on ignition of aluminium particles. *Combust. Theor. Model.*, **10**, 603–623.
- Wang, L., Luss, D., and Martirosyan, K.S. 2011. The behavior of nanothermite reaction based on Bi₂O₃/Al. *J. Appl. Phys.*, **110**, 074311.
- Williams, R.A., Patel, J.V., Ermoline, A., Schoenitz, M., and Dreizin, E.L. 2013. Correlation of optical emission and pressure generated upon ignition of fully-dense nanocomposite thermite powders. *Combust. Flame*, **160**, 734–741.
- Williams, R.A., Schoenitz, M., Ermoline, A., and Dreizin, E.L. 2012. On gas release by thermally-initiated fully-dense 2Al:3CuO nanocomposite powder. *Int. J. Energetic Mater. Chem. Propul.*, **11**, 275–292.
- Zhdanov, V.P., and Kasemo, B. 2008. Cabrera-Mott kinetics of oxidation of nm-sized metal particles. *Chem. Phys. Lett.*, **452**, 285–288.
- Zhou, L., Piekielek, N., Chowdhury, S., Lee, D., and Zachariah, M.R. 2009a. Transient ion ejection during nanocomposite thermite reactions. *J. Appl. Phys.*, **106**, 083306.
- Zhou, L., Piekielek, N., Chowdhury, S., and Zachariah, M.R. 2009b. T-Jump/time-of-flight mass spectrometry for time-resolved analysis of energetic materials. *Rapid Commun. Mass Spectrom.*, **23**, 194–202.
- Zhou, L., Piekielek, N., Chowdhury, S., and Zachariah, M.R. 2010. Time-resolved mass spectrometry of the exothermic reaction between nanoaluminum and metal oxides: The role of oxygen release. *J. Phys. Chem. C*, **114**, 14269–14275.